`Vol. 5, No. 3, pp. 351-371, (September 2024)
DOI: 10.21608/aujes.2024.298048.1256
Aswan University Journal of Environmental Studies (AUJES)
Online ISSN: 2735-4237, Print ISSN: 2735-4229
Journal homepage: https://aujes.journals.ekb.eg/ E-mail: AUJES@aswu.edu.eg
Original research

Novel Eco-Friendly Curcumin Pentamethine Cyanine Dyes as Photosensitizers and Antitumor

Naglaa S. El-Deen[1*], Sara M. Gamea[1], Reda M. Abd El-Aal[2], Ahmed I. Koraiem[1], Hussien A. Eldamarany[1]

[1] Department of Chemistry, Faculty of Science, Aswan University, 81528, Aswan, Egypt
[2] Department of Chemistry, Faculty of Science, Suez University,43512, Suez, Egypt

Received: 18/6/2024 Accepted: 14/7/2024

Abstract:

The aim of the recent study is creating and development more novel effectively and eco-friendly synthesis cyanine dyes based on extracted curcumin as a natural product compound **(1)** using as a primary essential intermediate through the preparation of some novel pentamethine **(2a-d), (4a-d)** respectively. Pentamethine cyanines with altered methine bridges were created by substituting curcumin connectors. Optical properties of the prepared dyes including, hydrophobic behavior in polar buffer solution, acidochromic manner, and molar absorptivity were measured. Cytotoxic activity results showed clearly that compounds **(1, 2c** and **2d)** had encouraging antitumor effect *in vitro* against two different anticancer cell lines of (prostate PC-3 & breast MCF-7), so, **(1), (2c), (2d),** showed variable cytotoxic effectively at IC_{50} (**17.76±1.4, 24.86±1.7, 51.67±2.8)** µM, respectively, against (PC-3), and at IC_{50} (**5.81±0.4, 9.12±0.7, 19.67±1.6)** µM respectively, against (MCF-7). The objective of the anticancer study of the prepared pentamethine cyanine dyes for application as an *in vivo* study in the future. Using elemental analysis and spectral investigations like (UV/Visible, IR, ^{1}H-NMR, and MS), the structure of new dyes was verified.

Keywords: Extraction, Curcumin, Synthesis, Chloroformyl curcumin, Cyanine dyes, Solvato-chromism, Acidochromic behavior, Antitumor activity.

1- Introduction

Curcumin has been demonstrated to be a strong anticancer (**Bolat et al., 2020; Harimurti et al., 2019**; **Luo et al., 2021)**, antioxidant (**Jakubczyk et al., 2020; Gel et al., 2018**), antimicrobial **(Papadimitriou et al., 2018; kumar Lawaniya**; **Goyal, 2022)**, antibacterial **(Bomdyal et al., 2017; Oghenejobo**; **Bethel, 2017 ; Oghenejobo et al., 2022)**, anti-inflammatory **(Fadus et al., 2017; Peng et al., 2021; Edwards et al., 2017)**, pharmaceutical **(Urošević et al., 2022; Suresh**; **Nangia, 2018; Ma et al., 2019; Kotha**; **Luthria, 2019),** antibiotics **(Teow**; **Ali, 2015; Itzia Azucena et al., 2019; Marini et al., 2018)** and photosensitizers **(Kazantzis et al., 2020; Dias et al., 2020 ; Araújo et al., 2017; Ghann et al., 2017)**.

Corresponding author*: E-mail address: naglaanaglaa@yahoo.com

Cyanine dyes have been the subject of increased scientific interest over the past ten years because of their many uses in the realms of biological, analytical, and biomedical research **(Lee et al., 2008)**. This large group of dyes differs from other dyes in that they have two heterocycles that contain nitrogen joined via a methine bridge that is conjugated. **(Patonay et al., 2004; Narayanan**; **Patonay, 1995; Flanagan et al., 1997)**. Cyanines exhibit a broad spectrum of absorption and fluorescence from the visible to infrared spectrum due to the heterocycles' dual roles as electron donors and acceptors, which results in an electron-deficient system throughout the molecule. Their high extinction coefficients and narrow absorption bands define them. **(Kobayashi et al., 2010)**. These special qualities, together with curcumin green's outstanding safety record in humans and the simplicity with which cyanines can be changed, have made the dyes useful for a wide range of applications. **(Zhang et al., 2016; Bellinger et al., 2018; Lyu et al., 2019)**. In particular, cyanine dyes that absorb and fluoresce near-infrared (NIR) have drawn interest in biological imaging. **(Hyun et al., 2014 and 2015; Wada et al., 2015; Njiojob et al., 2015)**, in dye-sensitized solar cells (DSSCs) to enable utilization of the red/near-IR portion of the solar spectrum due to the minimal background signal in this spectral region. **(Otsuka et al., 2008; Pitigala et al., 2016)**. For numerous pharmacological and biological processes, cyanine dyes are essential, including, antiproliferative **(Poreba et al., 2002)**, antiviral **(Azevedo et al., 2002)** cyclin-dependent kinase-inhibiting **(Misra et al., 2003)**, cardiovascular **(Stasch et al., 2002)**, antimalarial **(Menezes et al., 2002),** antileishmanial activities **(Mello et al., 2004)**, antimicrobial **(Goda. et al., 2004)**, inhibitors for cell growth and division **(Gilman et al., 1981; Uchiumi**; **Yasui**, **1979).** Also, cyanine dyes as antitumor (anti-cancer) agents **(Fadda et al., 2021; Gizem Özkan et al., 2021; Sabry et al., 2022)**.

In this recent research, our goal to prepare some novel photosensitizer dyes based on curcumin as effective natural chemical compound having safe different applications.

2- Materials and Methods

2.1. Materials:

General information

Solvents and chemicals were of American Chemical Society grade standards or HPLC purity used exactly as supplied. The source of the chemicals was Sigma-Aldrich (Saint Louis, MO), Fisher Scientific (Pittsburgh, PA, USA), and Across Organics.

2.2. Experimental and methods

Every melting point is not adjusted. The Micro Analytical Center, in Cairo-University, performed elemental analysis. The Perkin Elmer Infrared 127ß spectrophotometer, in Cairo-University, was used to determine the Infra-Red (KBr) spectra. A Bruker AMX-250 spectrometer was used to record the ^{1}H-NMR spectra. Using a HpMs 6988 spectrometer (Cairo University), Mass spectra were captured. 6405 UV/Visible recording spectrophotometer in Aswan, at the Faculty of Science, was used to record the visible absorption spectra wavelengths of the prepared dyes ranging from 350 to 700 nm. Through the Holding Company for Biological Products and Vaccines (VACSERA), Faculty of Pharmacy, Mansoura, the anticancer activities were documented from ATCC.

2.2.1. Extraction and isolation of Curcumin or (1,7-bis(4-hydroxy-3-methoxyphenyl) hepta-1,6-diene) (1)

Isolation of curcumin is worked according to **(Nurjanah et al., 2019, Perko et al., 2015; Yuvapriya et al., 2015)**. After being cleansed, rinsed under running water, the turmeric was allowed to air dry at R.T. The turmeric was ground into a powder after being crushed. A 250 g of powdered turmeric was

soaked in methyl alcohol as solvent overnight; When the solvent stopped turning orange, the extraction was terminated. The outcomes were compared after being filtered and concentrated with a rotary evaporator. Column chromatography on silica gel using dichloro-methane-methanol (97:3) % as the mobile phase was used to perform the isolation. Purity of extracted compound is indicated by TLC (thin-layer chromatography) method, Figure 1 (a), (b). Curcumin **(1)** structure was verified using elemental analysis, and spectral data of (IR, ^{1}H-NMR, and MS spectra). Molecular formula $C_{21}H_{20}O_6$, Mol. Wt.= 268; Calculated (Found) % C: 68.48 (68.40), H: 5.34 (5.28), N: 26.1 (26.0). Mass spectrum at *m/z*= 367 [M-1]. Thus, IR spectrum (KBr, cm^{-1}) for compound **(1)** reveals the presence of absorption bands at 2929.4 cm^{-1} (CH_3O), 3502.0 cm^{-1}(OH), 1509.1 cm^{-1} (C═C), a peculiar band at 1629.5 cm^{-1} (C═O). ^{1}H-NMR (DMSO, 400 MHz) spectrum of compound **(1)** exhibits signals at: δ (ppm) 2.51 (s, 2H, CH_2), 3.83 (s, 6H, 2 methoxy groups), 9.68 (s, 2H, 2 OH), 6.33 (d, 2H, 2 methine groups), 6.57 (d, 2H, 2 methine groups), 7.15 (d, 2H, Aromatic H), 7.37 (d, 2H, Aromatic H), 7.84 (d, 2H, Aromatic H).

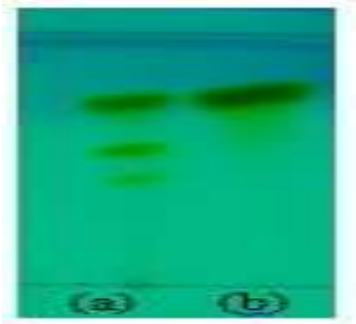

Fig 1: (a): TLC of plant extract**.** (b) TLC of isolated Curcumin.

2.2.2. Preparation of 1,7-bis(4-hydroxy-3-methoxyphenyl) hepta-1,4,6-triene-iodide -3,5[2(4) pentamethine cyanine dyes (2a-d).

(0.01M) of starting material **(1)** and (0.02 M) of N-methyl (2-picolinium, 4-picolinium, quinaldinium, and/or lepidinium) iodide were refluxed in an ethanolic solution, adding of a few drops of piperidine for eight hours. Filtration of the hot reaction mixture to remove any insoluble components. Concentration, cooling, and acidification with few drops of acetic acid was achifed to the filtrate. Pentamethine cyanine dyes **(2a-d),** were obtained after separation, filtration, and recrystallization the precipitated products followed by dilution with ice water, Table (1)**.**

2.2.3. Preparation of 5-chloro-3-oxo-1,7-bis(4-hydroxy-3-methoxyphenyl) hepta-1,6-diene-4-al (3)

According to **(Helliwell et al., 2006),** compound **(3)** is prepared. The precipitated product was greenish-gray colour, Yield= 60%; M.p = 120 **℃**. The chemical structure confirmation of **(3)** was done by elemental analysis, spectral data of (IR, ^{1}H-NMR, and MS spectra). Molecular formula **$C_{22}H_{21}O_6Cl$**, Mol. Wt.= 416.5; Calculated (Found) % C: 63.38 (63.37), H: 5.04 (5.01). Mass spectrum at *m/z*= 418.5 [M+2]. Thus, IR spectrum (KBr, cm^{-1}) for compound **(3)** reveals absorption bands at 3402 cm^{-1} (OH), 1509 cm^{-1} (C═C), and 1620, 1649 cm^{-1} (C═O), 2950 cm^{-1} (CHO). ^{1}H-NMR (DMSO, 400 MHz) spectrum of **(3)** reveals signals**:** at δ (ppm) 2.85 (s, 3H, methoxy group), 2.98 (s, 3H, methoxy group), 6.11- 7.19 (m, 12 H, Ar-H + olefinic protons), 8.15 (s, 1H, CHO).

2.2.4. Preparation of 1,7-bis(4-hydroxy-3-methoxyphenyl)-3-oxo- hepta-1,6-diene-iodide 4,5[2(4)] pentamethine cyanine dyes (4a-d)

Starting material **(3)** (0.01M) and 1-methyl (2-picolinium, 4-picolinium, quinaldinium, and/or lepidinium) iodide salts (0.02 M) were reacted, under piperidine / ethanol condition. The precipitated products **(4a-d),** Table (1), were separated in same manner for compounds **(2a-d).**

Table 1: Details on the novel prepared cyanine dyes' characteristics (2a-d), (4a-d).

Comp. No	color	Yield %	MP. ℃	Mol. Formula (Molecular Weight)	Calcd. % (Found) % C	H	N	λ_{max}(nm) in Ethanol	ε max (mol^{-1} cm^2)
2a	brown	70	140	$C_{35}H_{35}O_4N_2I$ (674)	62.31 (62.38)	5.19 (5.23)	4.15 (4.17)	425	11350
2b	brown	60	145	$C_{43}H_{39}O_4N_2I$ (774)	66.67 (66.70)	5.04 (5.07)	3.62 (3.60)	505(sh) 448 (sh) 422 (sh) 350	6160 14270 14130 21460
2c	brown	70	170	$C_{35}H_{35}O_4N_2I$ 674)	62.31 (61.35)	5.19 (5.21)	4.15 (4.19)	430	12170
2d	Deep brown	55	140	$C_{43}H_{39}O_4N_2I$ (774)	66.67 (66.65)	5.04 (5.05)	3.62 (3.65)	600(sh) 430	1500 24580
4a	brown	70	165	$C_{36}H_{35}O_5N_2I$ (702)	61.54 (61.58)	4.99 (5.02)	3.99 (4.01)	420	11470
4b	brown	70	150	$C_{44}H_{39}O_5N_2I$ (802)	65.84 (65.80)	4.86 (4.82)	3.49 (3.47)	512(sh) 465	8170 10800
4c	yellow	40	175	$C_{36}H_{35}O_5N_2I$ (702)	61.54 (61.52)	4.99 (5.96)	3.99 (4.02)	423	12880
4d	Deep brown	50	180	$C_{44}H_{39}O_5N_2I$ (802)	65.84 (65.82)	4.86 (4.84)	3.49 (3.45)	700 465(sh)	1420 4860

sh: shoulder of band

2.2.5 Stock solutions

By weighing the material in an amber vial using a 5-digit analytical balance and adding solvent with a class A volumetric pipette to achieve a final concentration of 1.0 mM, stock solutions of the dyes and standard were made. To guarantee total dissolution, the vials were sonicated for 15 minutes after being vortexed for 20 seconds. The stock solutions were kept at 4 °C in a dark freezer, when not in use. Just before usage, working solutions were made by diluting the stock to final concentrations.

2.2.5.1 The process for calculating molar absorptivity

Using a class A volumetric pipette, six ethanolic dilutions of dyes were prepared using stock solutions, in concentration range from 1 µM to 4 µM, to preserve absorbance between 0.0 and 2.5. Every sample's absorbance spectrum was measured in triplicate between 300 and 700 nm. The absorbance at the wavelength of maximum absorbance (λ_{max}) was calculated and each sample's absorbance at λ_{max} was plotted as a function of dye concentration to determine molar absorptivity. For several investigations, including solvatochromic and acidochromic behavior, the stock solutions were employed.

2.2.5.2 Spectral behavior studies in aqueous solutions of universal buffer

In a (10 ml) measuring flask, (5 ml) of the buffer solution and an exact volume of the stock solution were added. The mixture was then diluted to the correct level with redistilled water. Prior to performing spectral measurements, the pH of this solution was examined. For use in this experiment, a modified buffer series [pH = 2, 4, 5, 7, 8, 10, 13] was prepared, **(Shindy et al., 2021).**

2.2.6. Anticancer activity

2.2.6.1. Cell line and Chemical reagents

Human prostate cancer (PC-3) and the mammary gland cancer (MCF-7). Via the Holding Company for Biological Products and Vaccines (VACSERA), Cairo, Egypt, the cell line was obtained from ATCC. For comparison, doxorubicin was employed as a conventional anticancer medication. The reagents were Fetal Bovine serum (GIBCO, UK), MTT and DMSO (Sigma Co., St. Louis, USA), and RPMI-1640 medium.

2.2.6.1.1. Investigation of MTT (1)

The MTT investigation was utilized to determine the substances' inhibitory effects on cell growth. The basis of this colorimetric assay is the transformation of yellow tetrazolium bromide (MTT) by mitochondrial succinate dehydrogenase in living cells into a purple formazan derivative. 10% fetal bovine serum was added to RPMI-1640 media used to cultivate cell lines. At 37 ºC in an incubator with 5% CO_2, 100 units/ml of penicillin and 100µg/ml of streptomycin were introduced as antibiotics. The cell lines were seeded at 1.0x104 cells/well on a 96-well plate at 37 °C for 48 hours with 5% CO_2. Following incubation, the cells were exposed to several concentrations of chemicals and left for a full day of incubation. Following the medication treatment for 24 hours, 20 µl of MTT solution (5 mg/ml) was added, and the mixture was incubated for 4 hours. Each well receives 100 µl of dimethyl sulfoxide (DMSO) to dissolve the purple formazan that has developed. Using a plate reader (EXL 800, USA), the colorimetric test is measured and recorded at absorbance of 570 nm. (A570 of treated samples/A570 of untreated sample) X 100 was used to compute the relative cell viability as a percentage.

2.2.7. Ethical Approval Data:

Ethical Approval Code: ASWU/05/SC/ZO/24-07/M.Sc. 21
By: Research Ethics Committee at Faculty of Science, Aswan University.

3- Results and Discussion

3.1. Preparation

Pentamethine cyanines have been prepared via a condensation reaction between two salts of heterocyclic including quaternary nitrogen atom and a curcumin **(1),** followed by a dehydrohalogenation reaction of HI, as shown in **Schemes 1** and **2**. Under piperidine/ethanol conditions equimolar ratios of compound **(1)** react with bimolar ratios of N-methyl [2-picolinium, 4-picolinium, quinaldinium, and lepidinium] iodide to afford the corresponding **(2a-d)**, **Scheme 1.**

Pentamethine cyanine dyes **(4a-d), Scheme 2,** were prepared via formation of chloroformyl curcumin **(3)**. A Vilsmeier-Haack reagent is produced by reacting curcumin with phosphorous oxychloride and N, N-dimethylformamide to produce a linker **(3)**. Then, under piperidne/ ethanol condition, this linker **(3)** is condensed with salts of heterocyclic quaternary nitrogen atoms. Pentamethine cyanine dyes **(4a-d)** were proposed to be formed under simple conditions by a nucleophilic addition reaction between active carbonyl group of the compound **(3)** and the active methylene group of heterocyclic quaternary salt's, which was followed by the dehydrohalogenation of HCl and HI. The produced cyanine dyes of pentamethine, designated as **(2a-d)** and **(4a-d),** release iodine vapour when warmed with concentrated H_2SO_4 acid.

The structure of new dyes **(2a-d; 4a-d)** was confirmed by elemental analysis, Table (1), spectral data of (IR, ^{1}H -NMR, and Mass spectra)**.**

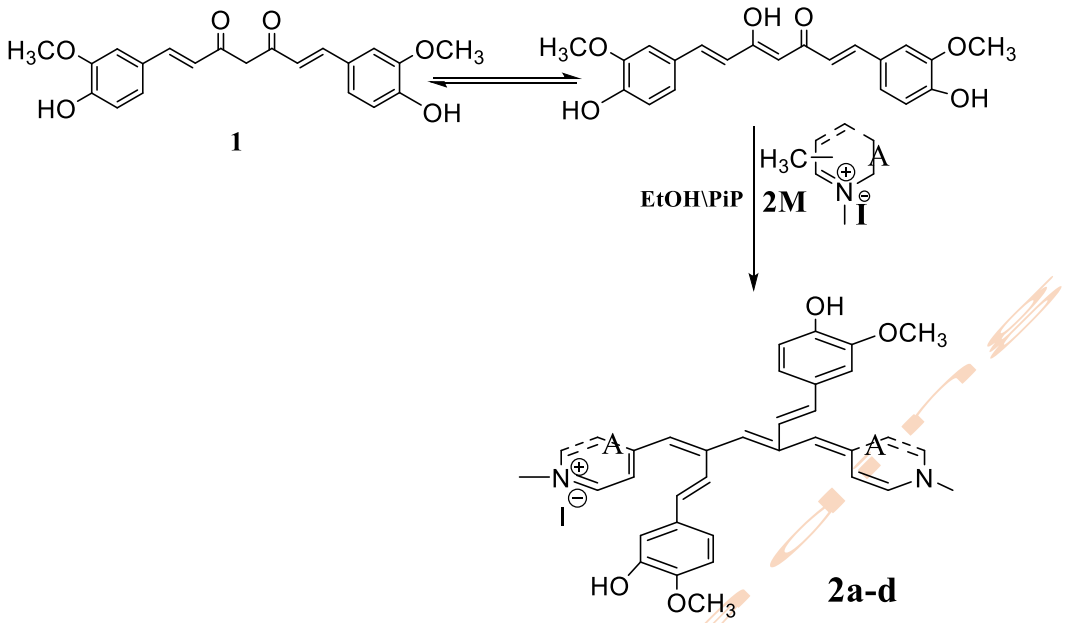

Scheme 1

(2a-d): A=N- methyl pyridin-2-ium iodide (a); A=N- methyl quinolin-2-ium iodide (b); A= N- methyl pyridin-4-ium iodide (c); A = N-methyl quinolin-4-ium iodide (d).

Thus, IR spectrum (KBr, cm^{-1}) for compound (**2c)** reveals general absorption bands at 2927 cm^{-1} (heterocyclic quaternary salt, $CH_3N^+I^-$ and CH_3O), 3352-3514 cm^{-1}(OH), 1495 cm^{-1}(C═N group), 1457-1635 cm^{-1}(C═C group). Meanwhile, compound **(4b)** in addition absorption bands for compound **(3)** reveals 1453.5 (C═N group), 2918 ($CH_3N^+I^-$), 2922 cm^{-1} (N-methyl heterocyclic). The EIMS revealed the peak of molecular ion for **(2c)** at *m/z* = 674 [M+2] & for **(4b)** at *m/z* = 804 [M+1].

3.2. Characteristics of optics

3.2.1. Spectral characteristics in Ethanol

For cyanine dyes to maintain their advantageous optical characteristics, structural modifications are necessary, that is why all of the compounds in **Schemes 1 & 2** their absorbance had been measured. Figures (2 and 3) show the variations in ethanol absorption that are produced by the type of heterocyclic residue A and the position of their connection. For the dyes with a pyridine **(2a)** and quinoline **(2b)** ring with the methine chain, respectively, Figure 2 shows that the λ_{max} ranges from 425 nm to 448 and 505 nm. Typically, the meso-carbonyl substitution or open chain pentamethine cyanines have a λ_{max} of approximately 700 nm. Absorption shifts in cyanines are usually found when alternate heterocycles with higher interaction with the conjugated system are used. **(Soriano et al., 2015)**. In compounds (**4b** & **4d)**, Figure (3), when the methine chain substitutions are changed, the most notable absorption shifts come from the alternate conjugation pathway in the meso-curcumin and the strain due to the changing in the linkage position of heterocyclic quaternary salts ring on the methine chain.

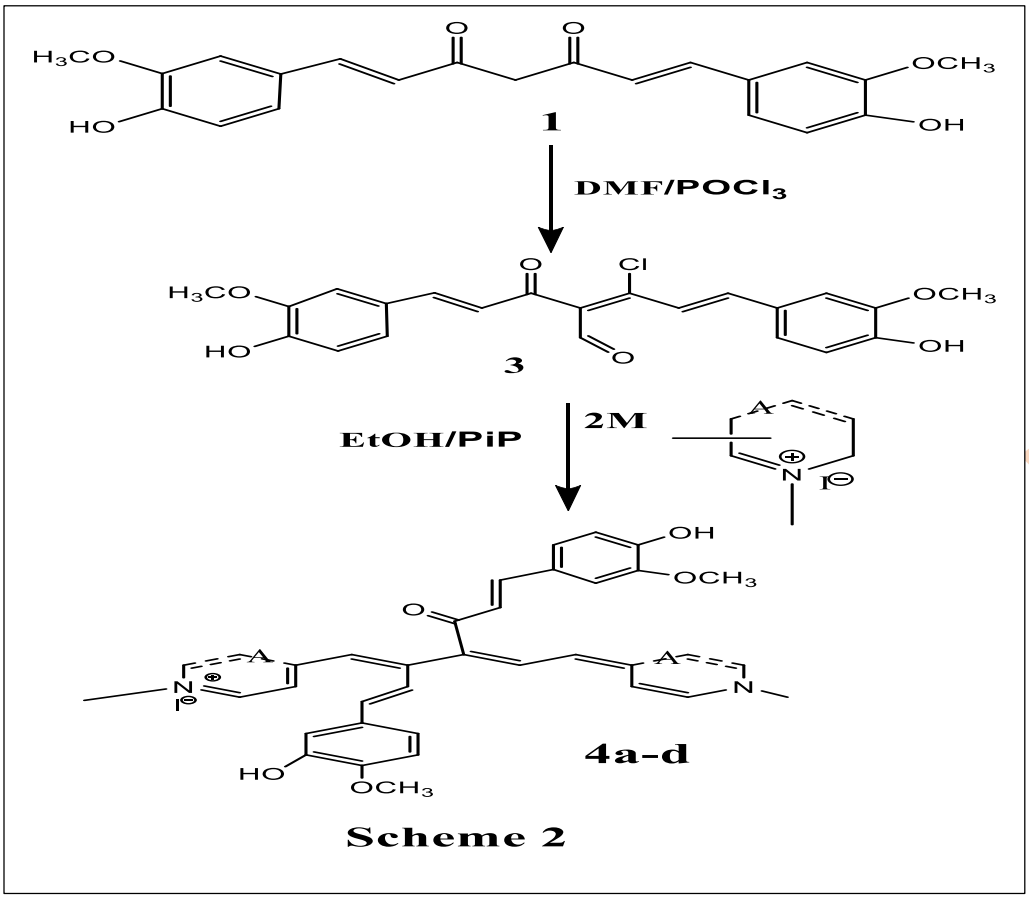

(4a-d): A= pyridin-2-ium iodide (a); A= N-Methyl quinolin-2-ium iodide (b); A= N-Methyl pyridin-4-ium iodide (c); A= N-Methyl quinolin-4-ium iodide (d).

The dyes' optical characteristics was been displayed in Table (1). These substances have molar absorptivity between 24850 and 26160. It's interesting to note that compounds (**2b** & **2d)**, which displayed molar absorptivity above 24 000, were also the ones that deviated most from the typical 350-430 nm absorbance maximum observed in pentamethine cyanines. The molar absorptivity can be increased by preventing cis-trans isomerization owing to the curcumin linker group in dyes (**2b** & **2d)** and the strain generated on the methine chain.

Notably, the compounds containing the meso-carbonyl group **(4b & 4d)** showed the lowest molar absorptivity. In contrast to the methine chain, the meso-carbonyl group may allow for more rotation at the C_2-C_3 link, Figure (4), which may lead to enhanced aggregation in polar liquids.

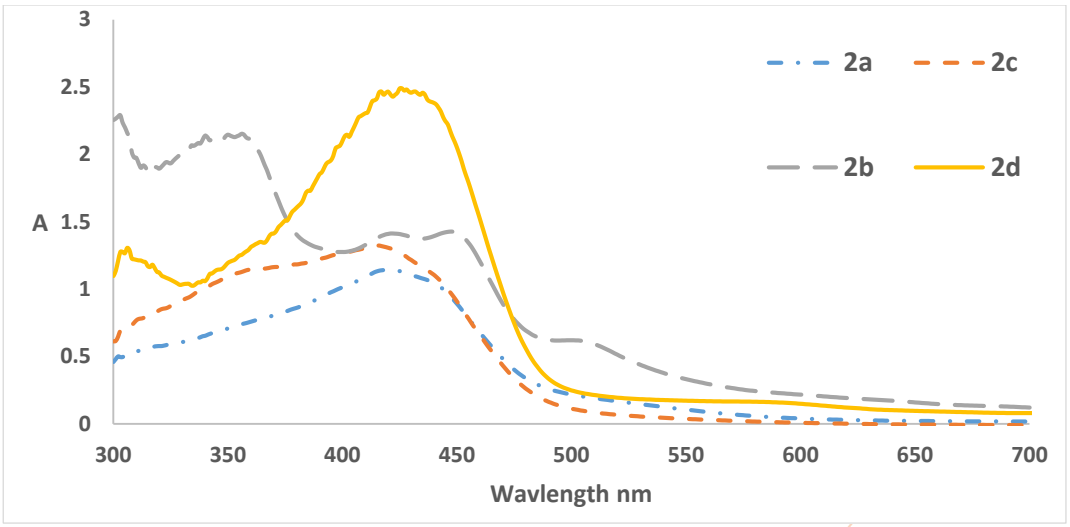

Fig. (2)**:** The visible electronic absorption spectra behavior of cyanine dyes in ethanol (**2a-d)**

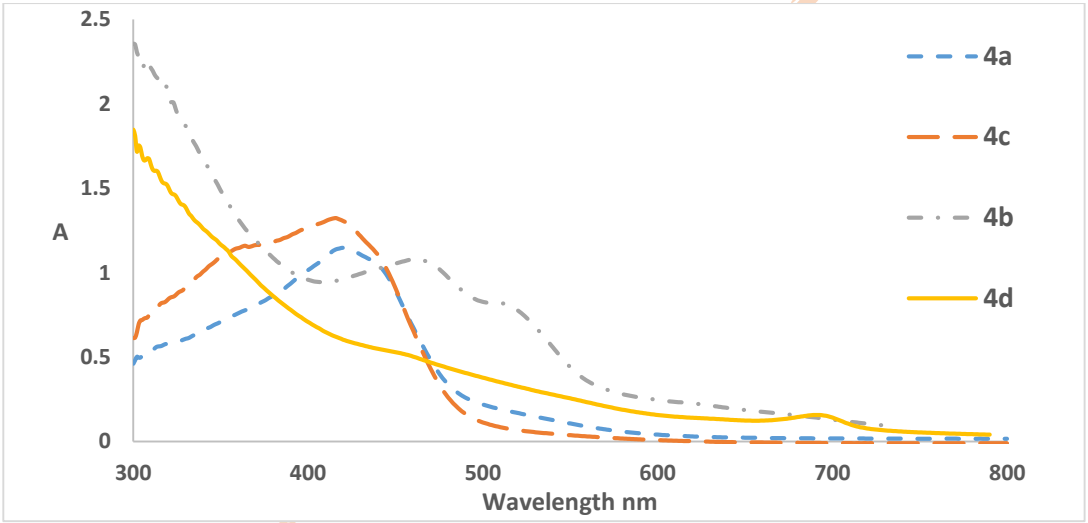

Fig. (3)**:** The visible electronic absorption spectra behavior of cyanine dyes in ethanol (**4a-d)**

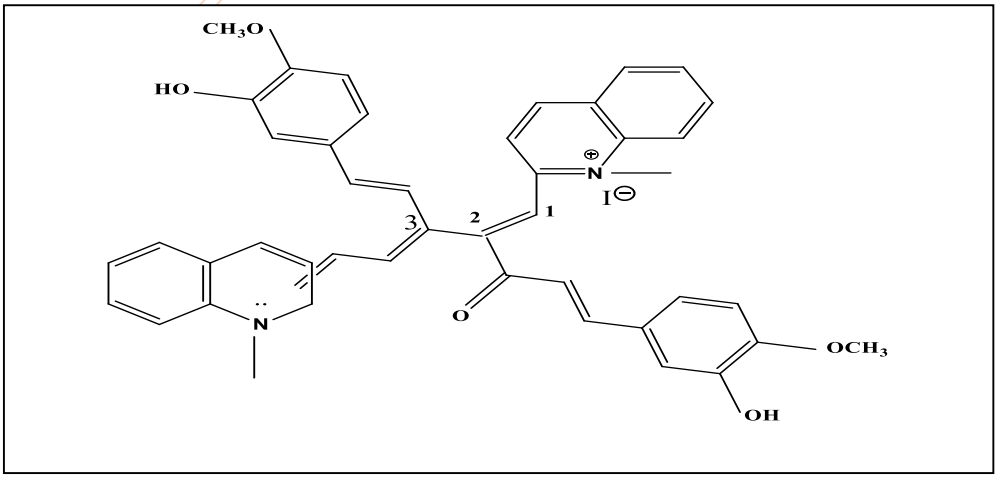

Fig. (4)**:** Opposite behavior of the methine chain leading to more rotation about the C_2–C_3 bond (**4b** & **4d)**

3.2.2. Studies of Photophysical behavior of cyanine Dyes curcumin selected

To investigate colorimetric and emission properties of synthesized probe pentamethine cyanine dyes **(2a & 4c)** was examined with various polarity indexes solvents such as **DMF, EtOH, DMS, CH_2Cl_2, $CHCl_3$, C_6H_6,** and **water**. For every solvent, the molar extinction coefficients were calculated at 1 X 10^{-5} M concentration. Which intramolecular charge transfer (ICT) is stimulated from the donor nitrogen lone pair of the heterocycle and the curcumin linker to the acceptor quaternary nitrogen of the other heterocycle depends on the solvent polarity. The purpose of its construction is to demonstrate the solvatochromic behavior of these dyes; Figures (5, 6), Table (2), and the intramolecular charge transfer band values (λ_{max} & ε_{max}) are provided. Depending on the dye type and structure, these dyes displayed increased solvent polarity and positive solvatochromism. This suggests that as the solvent's polarizability increases, the polar excited states of these cyanine dyes are sustained by polarization interaction forces.

These compounds' absorption spectra in variously polar organic solvents revealed hypsochromic alterations in ethanol with respect to **DMF** and **C_6H_6**. The primary cause of the bathochromic shift in **DMF** compared to **EtOH** is the rise in solvent polarity brought on by the former's increased dielectric constant. The solute-solvent interaction caused by the intermolecular hydrogen bonding between ethanol and the lone pair of electrons inside the heterocyclic ring structure produces the hypsochromic changes that are seen in **EtOH** with respect to **C_6H_6**. In the absence of this, the electron cloud's mobility along the conjugated pathway toward the positively charged center is reduced. It was important to note that the three bulk chorines' steric hindrance makes it difficult for **$CHCl_3$** molecules to form intermolecular hydrogen bonds with the lone pair of electrons of nitrogen or oxygen atoms in heterocyclic ring systems. Additionally, in the case of the **C_6H_6** solvent, the solute-solvent interactions left the nitrogen atoms of the heterocyclic ring system with a residual negative charge. This helped to facilitate the electronic charge transfer to the positively charged center and explains the bathochromic shifts in these solvents with respect to ethanol.

Properties of the acidic chromic were studied because the nitrogen atom of the quaternary ammonium salt and hydroxyl group in benzene ring they have a strong attraction for protons. These units probe demonstrated an acidochromic effect and explored the acid-sensing behavior of curcumin pentamethine cyanine dyes in solution medium.

Table (2): Absorption (λ nm) & extinction coefficients (ε mol^{-1} cm^{-1}) values of pentamethine cyanines (2a &4c) in different polar organic solvents

Comp N0.	H_2O		DMF		EtOH		DMS		DCM		$CHCl_3$		C_6H_6	
	λ	ε	λ	ε	λ	ε	λ	ε	λ	ε	λ	ε	λ	ε
2a	379(sh) 359(sh)	6640 6610	430	15200	423	11420	429	11130	427	13960	425	10030	423	10320
4c	317(sh)	10500	357	7240	328 (sh)	10440	355	3820	355	4550	358	71100	358	4190

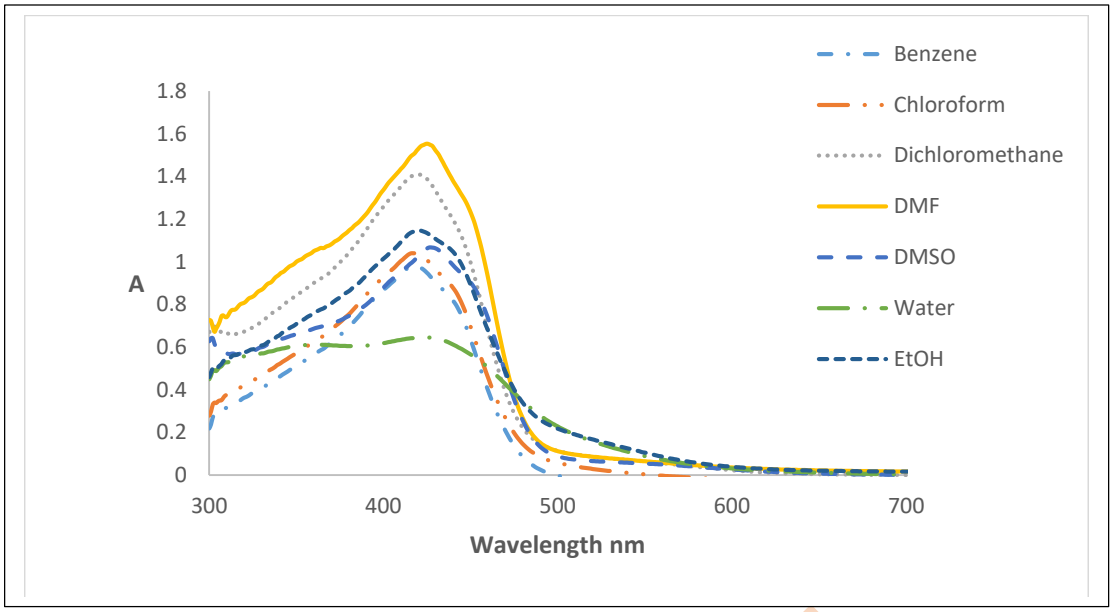

Fig. (5)**:** Solvatochromic spectra of compound **2a**

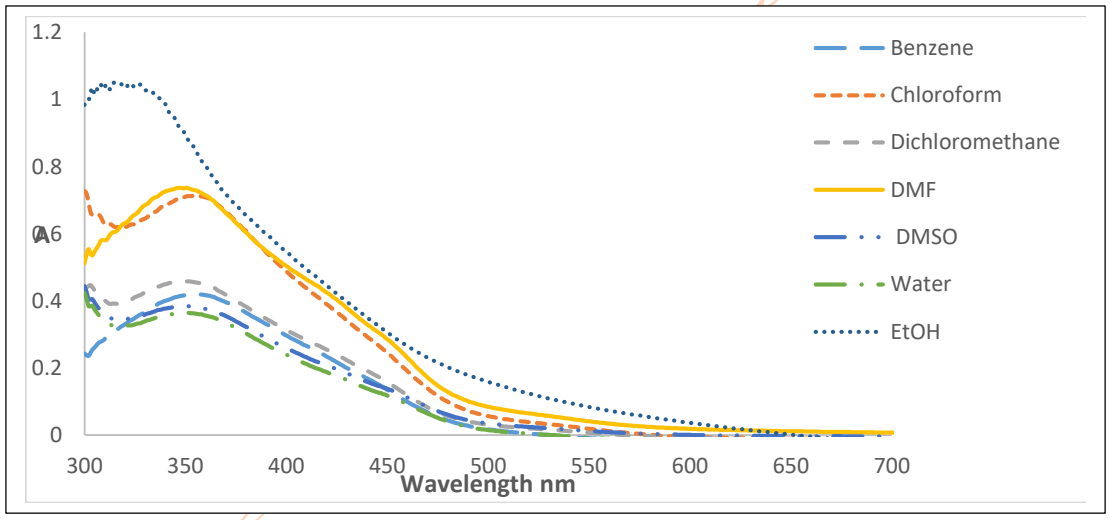

Fig. (6): Solvatochromic spectra of compound **4c**

3.2.3. Acidochromic behavior of new synthesized cyanines (2c) & (4d)

Certain pentamethine cyanine dyes **(2c)** & **(4d)** in ethanolic solution provide a persistent color in basic media that is released upon acidification. This encouraged us to investigate their spectral behavior in several aqueous universal buffer solutions to ascertain their pka values and to guarantee the ideal pH for applying these dyes as photosensitizers. When the compounds are present in the non-protonated, ionic forms with increased planarity, their efficacy as photosensitizers increases **(Mahmoud et al., 1975).** In aqueous universal buffer solutions with varied pH values (2, 4, 5, 7, 8, 10, and 13), the absorption spectra of the chosen dyes exhibited bathochromic shifts, with the absorption bands intensifying at high pH values (alkaline media), particularly in the n-π* and C.T. bands. In contrast, Table (3), Figures (7 & 8) show hypsochromic shifts with decreasing the intensity of the absorption bands at low pH values (acidic media).

Compounds **(2c)** & **(4d)** had distinct spectral behaviors when dissolved in either 95% ethanol or an aqueous universal buffer solution. Compound **(2c)** absorbed violet light at λ_{max} = 422 nm, whereas compound **(4d)** extended near violet light to λ_{max} = (315-708) nm. When these dyes are dissolved in an aqueous universal buffer solution, they absorb violet light (λ_{max} = 410 nm for compound **(2c)** at pH=2, which is bathochromic and hypsochromic shifted, and red light (λ_{max} = 703 nm for compound **(4d)**. The violet light's hypsochromic shift at pH=2 is caused by quinolinium methyl iodide, which acts as a strong inductive group and, to some extent, increases the bis pyrazolo type resonance. This causes the bis pyrazolo nitrogen atom in such a low pH solution to become protonated, which inhibits interaction and prevents the protonated form from absorbing energy in the visible spectrum. Additionally, intramolecular charge transfer (ICT) between the heterocyclic donor nitrogen and the heterocyclic acceptor nitrogen atoms is prevented, and the long wave length CT band vanishes. It is possible to attribute the observed new short wave length band to a localized π-η∗ transition. However, when the medium's pH rises, the protonated compound deprotonates, increasing its mesmeric interaction with the remaining molecules and, as a result, facilitating the CT interaction within the free base, as shown in Figures (7 & 8). This results in the bathochromic shift that is observed.

By varying the absorbance with pH values, one can use spectrophotometry to determine the dissociation and protonation constants (pka) values of such dyes **(2c & 4d) (Al-Basiouni, 1960).** Thus, using the spectrophotometric half-light limiting absorbance and collector methods, the absorbance pH curves represent the usual dissociation constant (pka) of dyes, which was found from the fluctuation of absorbance with pH **(Issa et al., 1969).** *S*-shaped curves were produced when the absorbance at a fixed wave number was plotted against pH values. The basic form of the dye was represented by the higher portion to the right of all *S*-shaped curves, while the acidic form was represented by the horizontal portion to the left. Given that the pH value at which half of the dye is in the basic form and the other half is in the acidic form is known as the pka value. The intersection of the *S*-curve and the horizontal line, halfway between the left and right segments, yielded this pka value. **(Ewing et al., 1960),** Figures (7& 8).

The dyes' protonated forms' spectrum properties and pka values **(2c** & **4d)** are collected in Table (4)**.** Thus, it was obvious that pka value reveals **(2c**, pka =4, 7, 10**)**, **(4d**, pka =4, 8**).** Thus, it was suggested that the **(2c** & **4d)** are more responsive in basic and acidic media as photosensitizers.

Table (3): Characterization values of the two synthesized cyanine dyes (2c & 4d) in different buffer universal solutions

Comp no	In 95% EtOH		In universal Buffer													
			2		4		5		7		8		10		13	
	λ_{max}	ε max Cm^{-1} mol^{-1}	λ_{max}	ε max Cm^{-1} mol^{-1}	λ_{max}	ε max Cm^{-1} mol^{-1}	λ_{max}	ε max Cm^{-1} mol^{-1}	λ_{max}	ε max Cm^{-1} mol^{-1}	λ_{max}	ε max Cm^{-1} mol^{-1}	λ_{max}	ε max Cm^{-1} mol^{-1}	λ_{max}	ε max Cm^{-1} mol^{-1}
2c	422	12960	410 (sh) 357 (sh) 317 (sh)	8220 8340 12080	422(sh) 362	13640 16080	420(sh) 360	18570 21770	417 (sh) 363	16500 18540	422	13630	410	20750	456	9940
4d	708 315(sh)	1470 16840	458 (sh) 313 (sh)	2950 13120	696	1480	701 312(sh)	1040 9960	703	1600	703 307 (sh)	2020 10360	703 413 (sh)	1150 4010	704 396 (sh)	1360 6000

Table (4): The absorbance variation at characteristic wavelength (λ_{max}) for two cyanines (2c & 4d) in different universal buffer solution

PH \ Comp. No. λ_{max}	Absorbance	
	2c	**4 d**
	λ_{max} (390)	**λ_{max} (700)**
2	0.85	0.087
4	1.44	0.134
5	1.967	0.104
7	1.707	0.163
8	1.358	0.204
10	2.376	0.116
13	0.773	0.144
P_{ka}	4 7 10	4 8

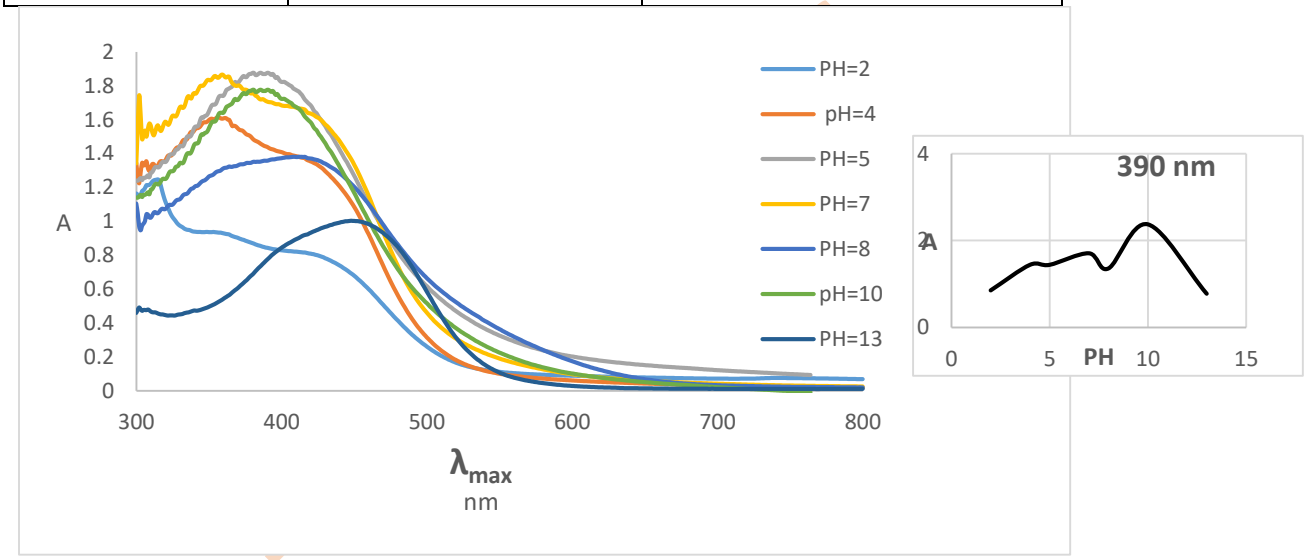

Fig. (7): The visible absorption spectra & *S*-curve absorption variation in universal buffer solution of compound **2c**

3.3. Anticancer effectivity

In an effort to create novel anticancer drugs, the novel cyanine dyes **(2a-d& 4a-d)** were designed and prepared. The anti-proliferative effect of some selected prepared dyes and their starting materials was assessed *in vitro* versus to (MCF-7 & PC-3) cell lines **(Metwally et al., 2012; Hossan; Abu-Melha, 2014; Eissa et al., 2016, Shaaban et al., 2015; Bondock et al., 2012; Etaiw et al., 2018; El-Helby et al., 2019; Sabry et al., 2022; Hamama et al., 2017).**

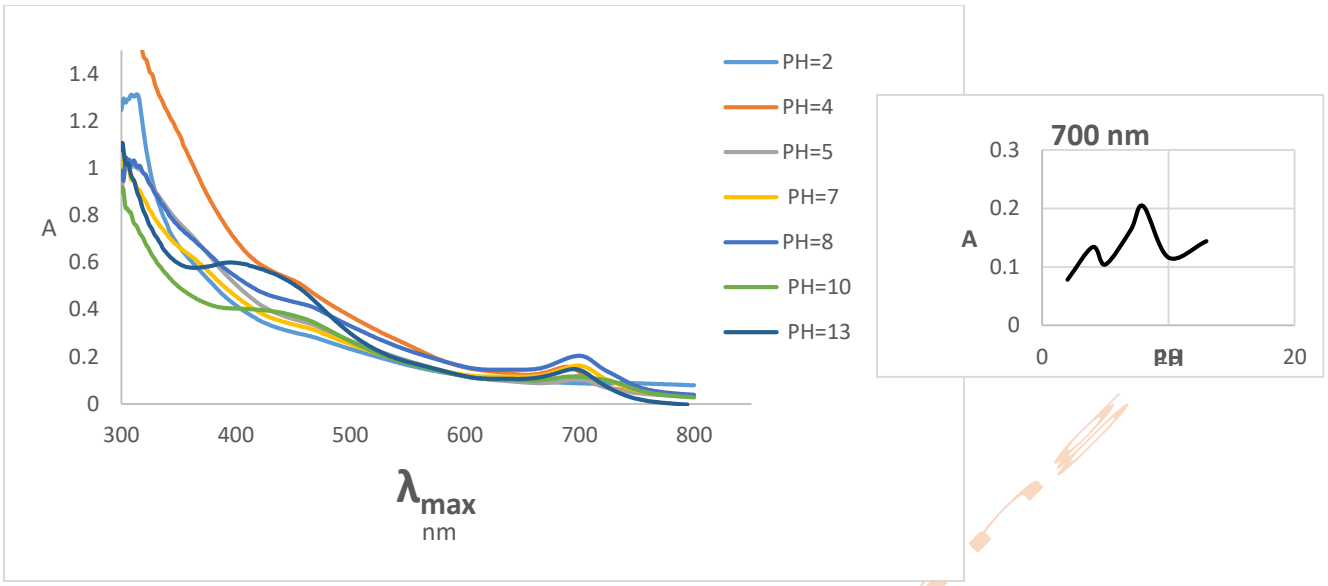

Fig. (8): The visible absorption spectra & *S*-curve absorption variation in universal buffer solution of compound **4d**

3.3.1. Anticancer consideration & cytotoxicity

Studying on the structure-anticancer activity relationship for some selected compounds of **(1), (2b), (2c), (2d), (3)** and **(4b)** to be evaluated for their *in vitro* anticancer effect including the conventional MTT technique **(Mosmann, 1983; Denizot et al., 1986; Thabrew et al., 1997),** against a panel of two human tumor cell lines, the MCF-7 breast cancer cell line and the PC-3 human prostate cell line. Through the Holding firm for biological products and vaccines (VACSERA) in Cairo, Egypt, the cell lines were acquired from ATCC. Due to result comparison, DOX was employed as a conventional anticancer medication.

Results, showed that compounds **(1), (2b), (2c), (2d), (3)** and **(4b)** inhibited the proliferation of human prostate (PC-3) for compounds **(1), (2b), (2c), (2d**), Figure (11), for compounds **(3), (4b)**, Figure (13), and breast cancer (MCF-7) for compounds **(1), (2b), (2c), (2d**), Figure (12), for compounds **(3), (4b)**, Figure (14), with various values, which increased in an orderly fashion.

Doxorubicin is used as standard anticancer drug toward (PC-3) cancer cell, which showed at IC_{50} (**8.87±0.6** µM), while toward (MCF-7) cancer cells, showed at IC_{50} **(4.17±0.2 µM**). Accordance of those values of Doxorubicin, thus, on compared the cytotoxic effect of the six examined prepared substances **(1, 2b, 2c, 2d, 3** and **4b)** versus to the (PC-3) cells, showed at IC_{50} (**17.76±1.4, 95.34±4.9, 24.86±1.7, 51.67±2.8, >100 and >100(**µM), respectively. The highest cytotoxicity was observed with **(1)** showing an IC_{50} of (**17.76±1** µM), followed by moderate cytotoxicity for **(2c),** IC_{50} of (**24.86±1.7)** µM, then weak cytotoxicity for **(2b), (2d**) with respective IC_{50} values of (**95.34±4.9, 51.67±2.8 (**µM). Finally, however non-cytotoxic effect for **(3), (4b)** with respective of IC_{50} (**>100** µM), Table (5); Figures (11, 12, 13, 14), **(Kamel et al., 2024).**

On the other hand, the six tested compounds **(1), (2b), (2c), (2d), (3) and (4b)** showed variable cytotoxic effectively against cells of (MCF-7) breast cancer, with IC_{50} (**5.81±0.4, 69.68±3.5, 9.12±0.7, 19.67±1.6, 78.58±3.9, 92.18±4.7)** µM respectively. Clearly, compound **(1)** should also be the strongest cytotoxicity toward (MCF-7) cancer cells with IC_{50} (**5.81±0.4**µM), followed by **(2c)**

IC_{50} (**9.12±0.7**µM), and **(2d)** (IC_{50} **19.67±1.6**µM), followed by weak cytotoxicity for compounds **(2b), (3), (4b)** for IC_{50}**, 69.68±3.5, 78.58±3.9, 92.18±4.7)** µM. Table (5); Figures (11, 12, 13, 14).

3.3.2. Cytotoxicity and structure relationship

In the current study, it is possible to correlate the structural properties of isolated compound **(1)**, and the related synthesized dyes to their cytotoxic activity. So, on comparison between the anticancer-activity of curcumin **(1)** and related pentamethine cyanine dyes ***(*2b, 2c** and **2d)** showed, that compound **(1)** has very strong activity versus to (MCF-7) and strong activity versus to (PC-3), due to that compound **(1)** has an active acidic character methylene group is in the middle of two electron withdrawing groups. On the other hand, pentamethine cyanine dye **(2c)** (A= pyridin-4-ium) showed very strong activity versus to (MCF-7) and moderate against (PC-3). On substitution of pentamethine cyanine dye ***(*2c) (**A= pyridin-4-ium) to **(2d)** (A= quinolium-4-ium), exhibited strong activity versus to (MCF-7) and weak against (PC-3), because of the extra phenyl ring in dye **(2d).** Additionally, on comparison between pentamethine cyanine dyes **(2b)** and **(2d),** it was found that dye **(2b)** (A= quinolium-2-ium), exhibited weak effectively versus to two (MCF-7) and (PC-3) while dye **(2d)** (A= quinolium-4-ium), exhibited strong effectively against (MCF-7) and weak against (PC-3). This is due to, the linkage position leading to increase π- conjugation in 4-ium link **(2d)** rather than quinolin-2-ium **(2b)** moieties, Table (5).

In comparison between curcumin **(1)** with related pentamethine cyanine dyes ***(*2b, 2c** and **2d),** it was obvious that compound **(1)** showed the highest anticancer-activities, Also, compound **(3)** and pentamethine cyanine dye **(4b)** show weak activity versus to (MCF-7) and non-effective against (PC-3), Table (5).

Table (5): Effective cytotoxic prepared compounds (1, 2b, 2c, 2d, 3 and 4b) versus (MCF-7) &(PC-3) **cell line**

No.	Comp.	*In vitro* Cytotoxicity IC_{50} (µM) •	
		PC-3	MCF-7
••	DOX	8.87±0.6	4.17±0.2
1	1	17.76±1.4	5.81±0.4
2	2b	95.34±4.9	69.68±3.5
3	2c	24.86±1.7	9.12±0.7
4	2d	51.67±2.8	19.67±1.6
5	3	>100	78.58±3.9
6	4b	>100	92.18±4.7

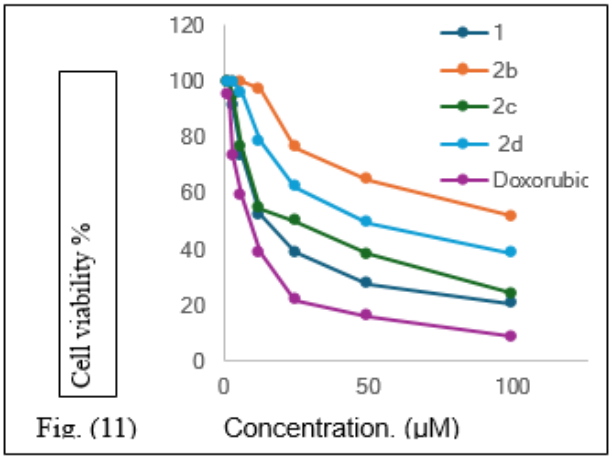

Fig. (11)

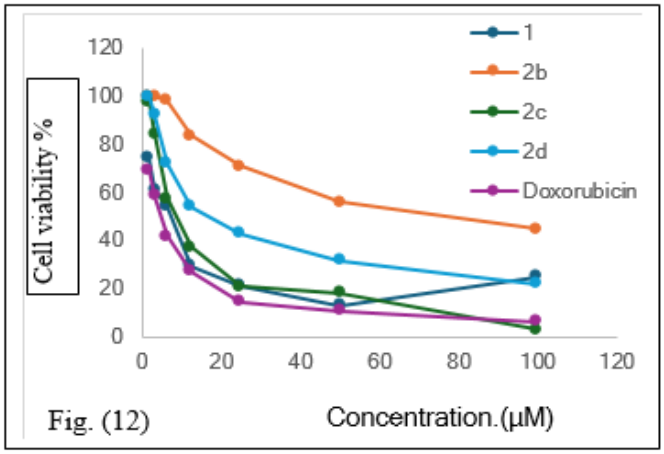

Fig. (12)

Fig. (11): Dose-response curve of the compounds **(1,2b,2c,2d, Dox)** toward **PC-3** cancer cells
Fig. (12): Dose-response curve of the compounds **(1,2b,2c,2d, Dox)** toward **MCF-7** cancer cells

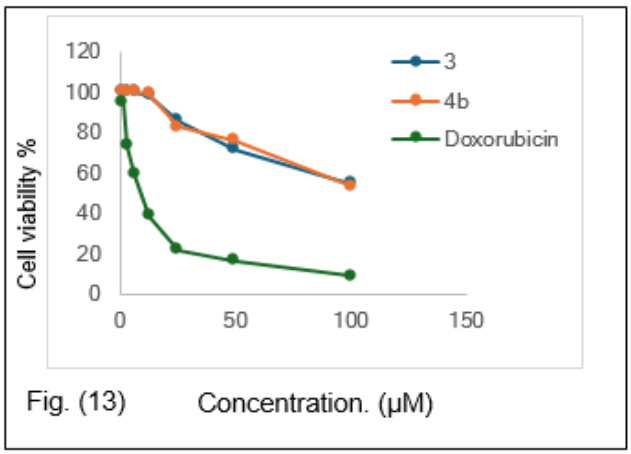

Fig. (13)

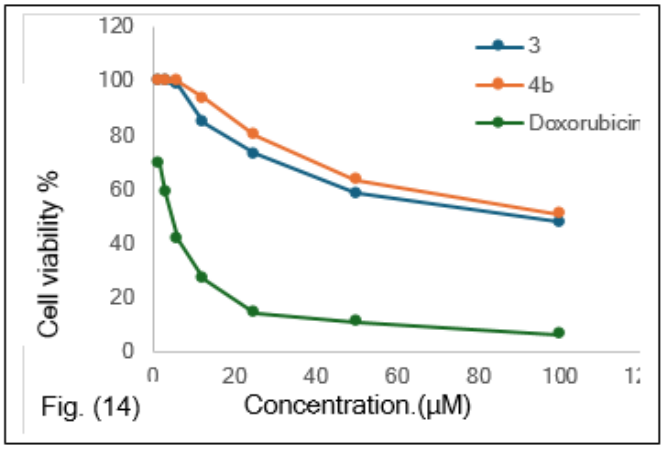

Fig. (14)

Fig. (13): Dose-response curve of the isolated compounds (3,4b, Dox) toward **PC-3** cancer cells.
Fig. (14): Dose-response curve of the isolated compounds (3,4b, Dox) toward **MCF-7**cancer cells.

4. Conclusion

This study is considered as new successful trend to use the extracted curcumin as a nature staring material to prepare some novel pentamethine cyanine dyes. The identification of these compounds was accomplished through the utilization of Infera-Red, ^{1}H-NMR, Mass spectra and elemental analysis. Also, spectral studies were conducted such as electronic visible absorption spectra, solvatochromic behaviour and acidochromic properties of the synthesized curcumin cyanines. We conducted *in vitro* assessments of chosen compounds to evaluate their properties, specifically focusing on their cytotoxic activities to know the extent of its anti-cancer effect on some cancer cells of Human prostate cancer (PC-3) and Mammary gland (MCF-7). Clearly, results of cytotoxic activities showed that compounds **(1, 2c, 2d)** exhibited favorable *in vitro* anticancer effectively versus to two different cell lines (PC-3 and MCF-7).

The highest cytotoxicity (strong) was observed with curcumin **(1)** versus to (PC-3) cancer cells showing at an IC_{50} of (**17.76±1** µM). Additionally, the increasing cytotoxicity versus to (MCF-7) cancer cells showing (very strong) for both **(1, 2c)** at an IC_{50} (**5.81±0.4**µM) for compound **(1)**, IC_{50} (**9.12±0.7**µM) compound **(2c)**, (strong) for **(2d)** and at an IC_{50} (**19.67±1.6**µM) for **(2d)**.

References

Agel, K. N., Abood, E., & Alsalim, T. (2018). Synthesis and antioxidant evaluation for monocarbonyl curcuminoids and their derivatives. *Innovaciencia*, *6*(2), 1-13.

Al-Basiouni, M. (1960). The Fundamentals of Art Education. *Dar Al-Maarif, Cairo*.

Azevedo, A. R., Ferreira, V. F., Mello, H. de, Leao-Ferreira, L. R., Jabor, A. V., Frugulhetti, I. C. P. P., Pereira, H. S., Moussatche, N. & Bernardino, A. M. R. (2002). Synthesis And Biological Evaluation of 1h-Pyrazolo[3,4- b]pyridine-5 Carboxylic Acids against Vaccinia Virus. *Heterocyclic Communications 8* (5), 427-732.

Araújo, N. C., De Menezes, R. F., Carneiro, V. S. M., dos Santos-Neto, A. P., Fontana, C. R., Bagnato, V.

S., & Gerbi, M. E. M. (2017). Photodynamic inactivation of cariogenic pathogens using curcumin as photosensitizer. *Photomedicine and laser surgery*, *35*(5), 259-263.

Bellinger, S., Hatamimoslehabadi, M., Borg, R. E., La, J., Catsoulis, P., Mithila, F., & Rochford, J. (2018). Characterization of a NIR absorbing thienyl curcumin contrast agent for photoacoustic imaging. *Chemical communications*, *54*(49), 6352-6355.

Bolat, Z. B., Islek, Z., Demir, B. N., Yilmaz, E. N., Sahin, F., & Ucisik, M. H. (2020). Curcumin-and piperine-loaded emulsomes as combinational treatment approach enhance the anticancer activity of curcumin on HCT116 colorectal cancer model. *Frontiers in bioengineering and biotechnology*, *8*, 50.

Bomdyal, R. S., Shah, M. U., Doshi, Y. S., Shah, V. A., & Khirade, S. P. (2017). Antibacterial activity of curcumin (turmeric) against periopathogens-An in vitro evaluation. *Journal of Advanced Clinical and Research Insights*, *4*(6), 175-180.

Bondock, S., Adel, S., Etman, H. A., & Badria, F. A. (2012). Synthesis and antitumor evaluation of some new 1, 3, 4-oxadiazole-based heterocycles. *European Journal of Medicinal Chemistry*, *48*, 192-199.

Denizot, F., Lang, R., (1986). Rapid colorimetric assay for cell growth and survival. Modifications to the tetrazolium dye procedure giving improved sensitivity and reliability. *J. Immunol, Methods 89*(2), 271-277.

Dias, L. D., Blanco, K. C., Mfouo-Tynga, I. S., Inada, N. M., & Bagnato, V. S. (2020). Curcumin as a photosensitizer: From molecular structure to recent advances in antimicrobial photodynamic therapy. *Journal of Photochemistry and Photobiology C: Photochemistry Reviews*, *45*, 100384.

Edwards, R. L., Luis, P. B., Varuzza, P. V., Joseph, A. I., Presley, S. H., Chaturvedi, R., & Schneider, C. (2017). The anti-inflammatory activity of curcumin is mediated by its oxidative metabolites. *Journal of Biological Chemistry*, *292*(52), 21243-21252.

Eissa, I. H., El-Naggar, A. M., & El-Hashash, M. A. (2016). Design, synthesis, molecular modeling and biological evaluation of novel 1H-pyrazolo [3, 4-b] pyridine derivatives as potential anticancer agents. *Bioorganic chemistry*, *67*, 43-56.

El-Helby, A. G. A., Sakr, H., Eissa, I. H., Abulkhair, H., Al-Karmalawy, A. A., & El-Adl, K. (2019). Design, synthesis, molecular docking, and anticancer activity of benzoxazole derivatives as VEGFR-2 inhibitors. *Archiv der Pharmazie*, *352*(10), 1900113.

Etaiw, S. E. D. H., Fayed, T. A., El-bendary, M. M., & Marie, H. (2018). Three-dimensional coordination polymers based on trimethyltin cation with nicotinic and isonicotinic acids as anticancer agents. *Applied Organometallic Chemistry*, *32*(2), e4066.

Ewing, G. E., Thompson, W. E., & Pimentel, G. C. (1960). Infrared detection of the formyl radical HCO. *The Journal of Chemical Physics*, *32*(3), 927-932.

Fadda, A. A., Tawfik, E. H., Abdel-Motaal, M., & Selim, Y. A. (2021). Synthesis of novel cyanine dye s as antitumor agents. *Archiv der Pharmazie*, *354*(3), 2000186.

Fadus, M. C., Lau, C., Bikhchandani, J., & Lynch, H. T. (2017). Curcumin: An age-old anti-inflammatory and anti-neoplastic agent. *Journal of traditional and complementary medicine*, *7*(3), 339- 346.

Flanagan, J. H., Khan, S. H., Menchen, S., Soper, S. A., & Hammer, R. P. (1997). Functionalized tricarbocyanine dyes as near-infrared fluorescent probes for biomolecules. *Bioconjugate chemistry*, *8*(5), 751-756.

Ghann, W., Kang, H., Emerson, E., Oh, J., Chavez-Gil, T., Nesbitt, F., & Uddin, J. (2017). Photophysical properties of near-IR cyanine dyes and their application as photosensitizers in dye sensitized solar cells. *Inorganica Chimica Acta*, *467*, 123-131.

Gilman. P. J.; Belly, R. T.; Koszelak, T. O.; zigman, S.; Us pat. 1980, 4, 232, 121; Chem. Abstract 94 (1981), 97109u.

Gizem Özkan, H., Toms, J., Maschauer, S., Prante, O., & Mokhir, A. (2021). Aminoferrocene-Based Anticancer Prodrugs Labelled with Cyanine Dyes for in vivo Imaging. *European Journal of Inorganic Chemistry*, *2021*(48), 5096-5102.

Goda, F. E., Abdel-Aziz, A. A.-M. & Atef, O. A. (2004). Synthesis, antimicrobial activity and conformational analysis of novel substituted pyridines: BF (3)-promoted reaction of hydrazine with 2-alkoxy pyridines. *Bioorganic Medicinal Chemistry 12*, 1845-1852.

Hamama, W. S., Ibrahim, M. E., Ghaith, E. A., & Zoorob, H. H. (2017). Peculiar reaction behavior of 1, 3-oxathiolan-5-one toward various reagents: Molecular modeling studies and in vitroantioxidant and cytotoxicity evaluation. *Synthetic Communications*, *47*(6), 566-580.

Harimurti, S., Nugroho, W. S., & Pramono, A. (2019). Energy Savings on Curcumine Derivative Gamavuton-0 Synthesis Using Microwave Irradiation. *Int J App Pharm*, *11*(3), 155-158.

Helliwell, M., Afgan, A., Baradarani, M. M., and Joule, J. A. (2006). Formylation of an indolenine 2-(diformylmethylidene)-3,3-dimethyl-2,3-dihydro-1H-indol. *Acta Cryst. 62*(2), o737–o738.

Hossan, A., & Abu-Melha, H. (2014). Synthesis, mass spectroscopic studies, cytotoxicity evaluation and quantitative structure activity relationship of novel isoindolin-1, 3-dione derivatives. *Synthesis, mass*, *21*.

Hyun, H., Park, M. H., Owens, E. A., Wada, H., Henary, M., Handgraaf, H. J., & Choi, H. S. (2015). Structure-inherent targeting of near-infrared fluorophores for parathyroid and thyroid gland imaging. *Nature medicine*, *21*(2), 192-197.

Hyun, H., Wada, H., Bao, K., Gravier, J., Yadav, Y., Laramie, M., & Choi, H. S. (2014). Phosphonated near-infrared fluorophores for biomedical imaging of bone. *Angewandte Chemie*, *126*(40), 10844-10848.

Issa, I. M., Issa, R. M., El-Ezabey, M. S., & Ahmed, Y. Z. (1969). Spectrophotometric Studies on Quinizarin Sulphonic Acid in Solutions of Varying pW. *Zeitschrift für Physikalische Chemie*, *242*(1), 169-176.

Itzia Azucena, R. C., José Roberto, C. L., Martin, Z. R., Rafael, C. Z., Leonardo, H. H., Gabriela, T. P., & Araceli, C. R. (2019). Drug susceptibility testing and synergistic antibacterial activity of curcumin with antibiotics against enterotoxigenic Escherichia coli. *Antibiotics*, *8*(2), 43.

Jakubczyk, K., Drużga, A., Katarzyna, J., & Skonieczna-Żydecka, K. (2020). Antioxidant potential of curcumin-A meta-analysis of randomized clinical trials. *Antioxidants*, *9*(11), 1092.

Kamel, N. M., Abdel-Motaal, F. F., El-Zayat, S. A., Mohamed, A. H., Ohta, S., Hussien, T. A.(2024). A New Secondary Metabolite with Antimicrobial, Antioxidant, and Cytotoxic Activities from an Endophytic Fungus, Gymnoascus thermotolerans. *Egyptian Journal of Botany*, *64* (1), 107-124.

Kazantzis, K. T., Koutsonikoli, K., Mavroidi, B., Zachariadis, M., Alexiou, P., Pelecanou, M., &

Sagnou, M. (2020). Curcumin derivatives as photosensitizers in photodynamic therapy: photophysical properties and in vitro studies with prostate cancer cells. *Photochemical & Photobiological Sciences*, *19*, 193-206

Kotha, R. R., & Luthria, D. L. (2019). Curcumin: biological, pharmaceutical, nutraceutical, and analytical aspects. *Molecules*, *24*(16), 2930.

Kobayashi, H., Ogawa, M., Alford, R., Choyke, P. L., & Urano, Y. (2010). New strategies for fluorescent probe design in medical diagnostic imaging. *Chemical reviews*, *110*(5), 2620-2640.

kumar Lawaniya, Y., & Goyal, P. K. (2022). Synthesis of Novel Indole-Curcumin Hybrids as Potential Antimicrobial Agents. *Chemical Science Review and Letters 11* (41), 104-110.

Lee, H., Mason, J. C., & Achilefu, S. (2008). Synthesis and spectral properties of near-infrared aminophenyl-, hydroxyphenyl-, and phenyl-substituted heptamethine cyanines. *The Journal of organic chemistry*, *73*(2), 723-725.

Luo, S. M., Wu, Y. P., Huang, L. C., Huang, S. M., & Hueng, D. Y. (2021). The anti-cancer effect of four curcumin analogues on human glioma cells. *OncoTargets and therapy*, 4345-4359.

Lyu, H., Wang, D., Cai, L., Wang, D. J., & Li, X. M. (2019). Synthesis, photophysical and solvatochromic properties of diacetoxyboron complexes with curcumin derivatives. *Spectrochimica Acta Part A: Molecular and Biomolecular Spectroscopy*, *220*, 117126.

Ma, Z., Wang, N., He, H., & Tang, X. (2019). Pharmaceutical strategies of improving oral systemic bioavailability of curcumin for clinical application. *Journal of Controlled Release*, *316*, 359-380.

Mahmoud, M. R.; Khalil, Z. H. & Issa, R. M. (1975). Spectrophotometric studies of some styryl cyanine dyes. *Acta. Chim.Acad. Sci. Hung*, *87*(2), 121-128.

Marini, E., Di Giulio, M., Magi, G., Di Lodovico, S., Cimarelli, M. E., Brenciani, A., & Facinelli, B. (2018). Curcumin, an antibiotic resistance breaker against a multiresistant clinical isolate of Mycobacterium abscessus. *Phytotherapy research*, *32*(3), 488-495.

Mello, H. De., Echevarria, A., Bernardino, A. M., Canto-Cavalheiro, M. & Leon, L. L. (2004). Antileishmanial Pyrazolopyridine Derivatives: Synthesis and Structure—Activity Relationship Analysis. *Journal of Medicinal Chemistry 47* (22), 5427-5432.

Menezes, C. M. S., Sant´Anna, C. M. R., Rangel Rodrigues C., & Barreiro, E. J. (2002). Molecular Modeling of New Derivatives 1H-Pyrazolo[3,4-b]pyridine Designed as Isosters of Antimalarial Mefloquine. *Journal of Molecular Structure: Theory and Computation in Chemistry 579*, 31-39.

Metwally, M. A., Gouda, M. A., Harmal, A. N., & Khalil, A. M. (2012). Synthesis, antitumor, cytotoxic and antioxidant evaluation of some new pyrazolotriazines attached to antipyrine moiety. *European journal of medicinal chemistry*, *56*, 254-262.

Misra, R. N., Xiao, H. Y, Rawlins, D. B., Shan, W., Kellar, K. A., Mulheron, J. G., Sack, J. S., Tokarski, J. S., Kimball, S. D.& Webster, K. R. (2003). 1H-pyrazolo[3,4-b]pyridine inhibitors of cyclin-dependant kinases. *Bioorganic Medicinal Chemistry Letters 13*, 2405-2408.

Mosmann, T., (1983). Rapid colorimetric assay for cellular growth and survival: application to proliferation and cytotoxicity assays. *J Immunol Methods, 65*(1-2),55-63.

Narayanan, N., & Patonay, G. (1995). A new method for the synthesis of heptamethine cyanine dyes: synthesis of new near-infrared fluorescent labels. *The Journal of Organic Chemistry*, *60*(8), 2391-2395.

Njiojob, C. N., Owens, E. A., Narayana, L., Hyun, H., Choi, H. S., & Henary, M. (2015). Tailored near-infrared contrast agents for image guided surgery. *Journal of medicinal chemistry*, *58*(6), 2845-2854.

Nurjanah, N., &Saepudin, E. (2019). AIP Conference Proceedings, *2168*, (1).

Oghenejobo, M., & Bethel, O. (2017). Antibacterial evaluation, phytochemical screening and ascorbic acid assay of turmeric (Curcuma longa). *MOJ Bioequiv Availab*, *4*(2), 00063.

Oghenejobo, M., Opajobi, O. A., Bethel, U. O., & Uzuegbu, U. E. (2022). Determination of Antibacterial Evaluation, Phytochemical Screening and Ascorbic Acid Assay of Turmeric (Curcuma longa). *Challenges and Advances in Pharmaceutical Research*, *1*, 146-161.

Otsuka, A., Funabiki, K., Sugiyama, N., Mase, H., Yoshida, T., Minoura, H., & Matsui, M. (2008). Design and synthesis of near-infrared-active Heptamethine–Cyanine dyes to suppress aggregation in a dye-sensitized porous zinc oxide solar cell. *Chemistry Letters*, *37*(2), 176-177.

Papadimitriou, A., Ketikidis, I., Stathopoulou, M. K., Banti, C. N., Papachristodoulou, C., Zoumpoulakis, L., & Hadjikakou, S. K. (2018). Innovative material containing the natural product curcumin, with enhanced antimicrobial properties for active packaging. *Materials Science and Engineering: C*, *84*, 118-122.

Patonay, G., Salon, J., Sowell, J., & Strekowski, L. (2004). Noncovalent labeling of biomolecules with red and near-infrared dyes. *Molecules*, *9*(3), 40-49.

Perko, T., Ravber, M., Knez, Ž., and Škerget, M.(2015). Isolation, characterization and formulation of curcuminoids and in vitro release study of the encapsulated particles. *Journal of Supercritical Fluids, 103*, 48-54.

Peng, Y., Ao, M., Dong, B., Jiang, Y., Yu, L., Chen, Z., & Xu, R. (2021). Anti-inflammatory effects of curcumin in the inflammatory diseases: Status, limitations and countermeasures. *Drug design, development and therapy*, 4503-4525.

Pitigala, P. D., Henary, M. M., Owens, E. A., UnilPerera, A. G., & Tennakone, K. (2016). Excitonic photovoltaic effect in a cyanine dye molecular assembly electronically coupled to n-and p-type semiconductors. *Journal of Photochemistry and Photobiology A: Chemistry*, *325*, 39-44.

Poreba, K., Opolski, A. & Wietrzyk, J. (2002). Synthesis and antiproliferative activity in vitro of new 3- substituted aminopyrazolo[3,4-b]pyridines. *Acta Poloniae Pharmaceutica 59* (3), 215-222.

Sabry, M. A., Ghaly, M. A., Maarouf, A. R., & El-Subbagh, H. I. (2022). New thiazole-based derivatives as EGFR/HER2 and DHFR inhibitors: Synthesis, molecular modeling simulations and anticancer activity. *European Journal of Medicinal Chemistry*, *241*, 114661.

Shaaban, S., Negm, A., Sobh, M. A., & Wessjohann, L. A. (2015). Organoselenocyanates and symmetrical diselenides redox modulators: Design, synthesis and biological evaluation. *European journal of medicinal chemistry*, *97*, 190-201.

Shindy, H., El-Maghraby, M., & Eissa, F. M. (2021). Solvatochromism and halochromism of some furo/pyrazole cyanine dyes. *HA Shindy, MA El-Maghraby and FM Eissa. Solvatochromism and Halochromism of Some Furo/Pyrazole Cyanine Dyes. Chemistry International*, *7*(1), 39-52.

Suresh, K., & Nangia, A. (2018). Curcumin: Pharmaceutical solids as a platform to improve solubility and bioavailability. *CrystEngComm*, *20*(24), 3277-3296.

Soriano, E., Holder, C., Levitz, A., & Henary, M. (2015). Benz [c, d] indolium-containing monomethine cyanine dyes: Synthesis and photophysical properties. *Molecules*, *21*(1), 23.

Stasch, J.-P., Dembowsky, K., Perzborn, E., Stahl, E. & Schramm, M. (2002), "Cardiovascular actions of a novel NO-independent guanylyl cyclase stimulator, BAY 41-8543: in vivo studies", British Journal of Pharmacolology 135 (2), 344-355.

Teow, S. Y., & Ali, S. A. (2015). Synergistic antibacterial activity of Curcumin with antibiotics against Staphylococcus aureus. *Pak. J. Pharm. Sci*, *28*(6), 2109-2114.

Thabrew, M.I., Hughes, R.D.& McFarlane, I.G. (1997). Screening of Hepatoprotective Plant Components using aHepG2 Cell Cytotoxicity Assay. *J. Pharm. Pharmacol.,49,*1132-1 135.

Wada, H., Hyun, H., Vargas, C., Gravier, J., Park, G., Gioux, S., & Choi, H. S. (2015). Pancreas-targeted NIR fluorophores for dual-channel image-guided abdominal surgery. *Theranostics*, *5*(1), 1.

Uchiumi, K; Yasui, S., Hiroshi (Japan Photosensitive Dyes Co L td) Japanes pat. 7915, 839, (1979), AppI. 78 63 481.

Urošević, M., Nikolić, L., Gajić, I., Nikolić, V., Dinić, A., & Miljković, V. (2022). Curcumin: Biological activities and modern pharmaceutical forms. *Antibiotics*, *11*(2), 135.

Yuvapriya, S., Chandramohan, M., and Muthukumaran, P.; *International Journal of Pharmaceutical Research & Allied Sciences*, *4*(2). (2015).

Zhang, J, Terrones, M., Rae Park, C., Mukherjee, R., Monthioux , M., Koratkar, N., Seung Kim, Y., Hurt, R., , Frackowiak E., , T Enoki , T., Chen, Y., Chen, Y., Bianco, A.(2016). Carbon science in 2016: Status, challenges and perspectives. *Carbon 98,* 708-732.